

Mass Transfer from an Oscillating Microsphere

Jiahua Zhu,* Feng Zheng,† Mary L. Laucks, and E. James Davis‡¹

*School of Chemical Engineering, Sichuan University, Chengdu, China; †Pacific Northwest National Laboratory, P.O. Box 999, MSIN K6-28, Richland, Washington 99352; and ‡Department of Chemical Engineering, University of Washington, Seattle, Washington 98195-1750

Received July 20, 2001; accepted February 7, 2002; published online April 10, 2002

The enhancement of mass transfer from single oscillating aerocolloidal droplets having initial diameters $\sim 40 \mu\text{m}$ has been measured using electrodynamic levitation to trap and oscillate a droplet evaporating in nitrogen gas. The frequency and amplitude of the oscillation were controlled by means of ac and dc fields applied to the ring electrodes of the electrodynamic balance (EDB). Elastic light scattering was used to size the droplet. It is shown that the mass transfer process for a colloidal or aerocolloidal particle oscillating in the Stokes flow regime is governed by a Peclet number for oscillation and a dimensionless oscillation parameter that represents the ratio of the diffusion time scale to the oscillation time scale. Evaporation rates are reported for stably oscillating droplets that are as much as five times the rate for evaporation in a stagnant gas. The enhancement is substantially larger than that predicted by quasi-steady-flow mass transfer. © 2002 Elsevier Science (USA)

Key Words: elastic light scattering; electrodynamic balance; evaporation, mass transfer; oscillation.

INTRODUCTION

Mass transfer between colloidal or aerocolloidal particles and the surrounding fluid or gas can be enhanced by oscillating the particles. Particle oscillation can be achieved by a variety of methods, including acoustic oscillation, electric field oscillation for charged particles, and magnetic field oscillation for magnetic particles. The mass transfer process considered here is aerocolloidal droplet evaporation.

Evaporative mass transfer from an aerosol droplet has been the object of numerous theoretical and experimental studies dating from Maxwell's (1) analysis of simultaneous heat and mass transfer from an evaporating droplet to a surrounding stagnant gas. Reviews of aerosol evaporation/condensation processes to or from stagnant gases have been published by Wagner (2) and Kulmala and Vesala (3). If the droplet is in motion relative to the surrounding gas, heat and mass transfer fluxes can be enhanced. Kronig and Bruijsten (4) analyzed heat and mass transfer between a sphere and a steady low Reynolds number flow, and Acrivos and Taylor (5) and Rimmer (6, 7) improved on the theory using the method of matched asymptotic expansions.

Rimmer's solution for the dimensionless mass transfer coefficient, the Sherwood number, as a function of the Peclet number, $Pe = 2au_\infty/D_{ij} = ReSc$, is

$$Sh = 2 + 0.5Pe + f(Sc)Pe^2 + 0.25Pe^2 \ln Pe + \dots, \quad [1]$$

in which the Schmidt number is $Sc = \nu/D_{ij}$, $Re = 2au_\infty/\nu$ is the Reynolds number, and

$$f(Sc) = -\frac{1}{4} \left[\frac{173}{160} + \ln 2 - \gamma - \frac{Sc^2}{2} + \frac{Sc}{4} - \left(1 + \frac{3}{2}Sc - \frac{Sc^3}{2} \right) \ln \left(1 + \frac{1}{Sc} \right) \right], \quad [2]$$

where γ is Euler's constant ($\gamma = 0.57722\dots$). Here the Sherwood number is $Sh = 2aK_G/D_{ij}$, in which K_G is the gas phase mass transfer coefficient, D_{ij} is the diffusivity of the vapor in the surrounding gas, u_∞ is the bulk gas velocity, a is the droplet radius, and ν is the kinematic viscosity of the gas.

The original result published by Rimmer was incorrect, but he published a correction the following year (7). In the limit $Sc \rightarrow \infty$, $f(Sc)$ reduces to 0.03404, which recovers the solution of Acrivos and Taylor.

Taffin and Davis (8) and Zhang and Davis (9) used electrodynamic levitation to hold a single droplet in a low Reynolds number gas stream, and they varied the gas flow rate to alter the Peclet number. Zhang and Davis proposed an interpolation formula based on the low-Pe asymptotic solution of Kronig and Bruijsten and the high-Pe solution of Levich (10). Their correlation has the form

$$Sh = 2 + \left[(0.5Pe + 0.3026Pe^2)^{-n} + (1.008Pe^{1/3})^{-n} \right]^{-1/n}, \quad [3]$$

which recovers the asymptotic limits for both high and low Pe. They found that the choice $n = 3$ agrees best with experimental data, but $n = 2$ agrees with data nearly as well. For $Pe < 1$ their data are in good agreement with the results of Acrivos and Taylor and Rimmer, but for $Pe > 1$ the theoretical solutions greatly exceed the measured mass transfer rate.

¹ To whom correspondence should be addressed.

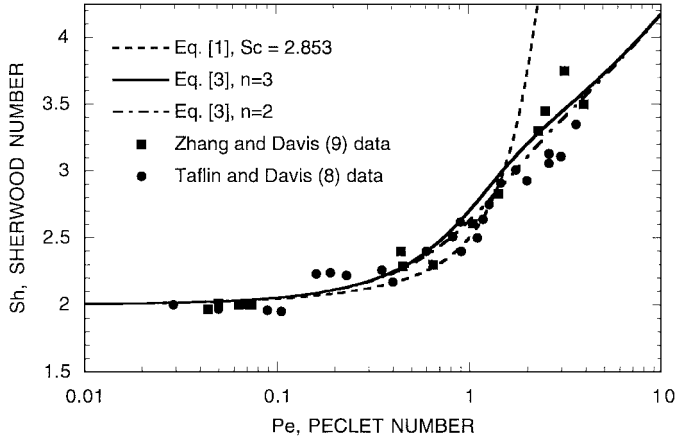


FIG. 1. A comparison between the Sherwood numbers calculated using Eqs. [1] and [3] and previously published data for steady flow.

To illustrate the effects of steady particle motion on the mass transfer process, Rimmer's equation and the interpolation formula of Zhang and Davis are compared with the experimental data of Taflin and Davis and Zhang and Davis in Fig. 1. Rimmer's theory fails for $Pe > 1$, and the data scatter around the interpolation formula given by Eq. [3] with $n = 2$ or 3 . We note that Eqs. [1] and [3] reduce to $Sh = 2$ for a stagnant surrounding medium, and for $Pe < 0.1$ Fig. 1 shows that there is very little effect of convection on the Sherwood number for steady flow of the surrounding fluid. For mass transfer in a stagnant medium the time rate of change of the particle mass, m , is given by the Maxwell (1) equation,

$$\frac{dm}{dt} = -\frac{4\pi a D_{ij} M_i}{R} \left[\frac{p_i^\circ(T_a)}{T_a} - \frac{p_\infty}{T_\infty} \right], \quad [4]$$

where R is the ideal gas constant, M_i is the molecular weight of the evaporating species, $p_i^\circ(T_a)$ is the vapor pressure of the evaporating species at the interfacial temperature, T_a , p_∞ is the partial pressure of the vapor in the bulk gas, and T_∞ is the temperature of the bulk gas. If the evaporation rate is sufficiently slow, the interfacial temperature remains very close to the bulk gas temperature. In this case, writing $m = 4\pi\rho a^3/3$, Eq. [4] can be integrated to obtain the droplet radius as a function of time to give

$$a^2 = a_0^2 - \frac{2D_{ij}M_i}{\rho RT_\infty} [p_i^\circ(T_\infty) - p_\infty](t - t_0). \quad [5]$$

Here ρ is the particle density. In this quasi-steady-state approximation a_0 is the particle radius at time t_0 . This result can be expected to give a lower limit on the evaporation rate for comparison with the effects of particle motion on the mass transfer.

Tian and Apfel (11) studied droplet evaporation by levitating single drops and arrays of drops using an acoustic field generated by a standing wave. Water drops and ethanol drops having

diameters of order 1 mm were charged to prevent coalescence. The number and size of drops were controlled by the amplitude of the acoustic vibration and the applied dc voltage. They found that their evaporation data agreed with Eq. [4] with the surface temperature given by

$$T_a = T_\infty - \frac{D_{ij}M_iL}{kR} \left[\frac{p_\infty}{T_\infty} - \frac{p(T_a)}{T_a} \right], \quad [6]$$

where L is the latent heat of vaporization, and k is the thermal conductivity of the gas.

The evaporation rate data for single drops were found to follow Eq. [5]; that is, the square of the radius was found to be a linear function of time. There was no appreciable effect of the streaming current on the evaporation rate. In their case, however, the streaming velocity was only of order 1 cm s^{-1} . Based on the Sherwood number equation given by Rosner (12),

$$Sh \approx 2(1 + 0.276Re^{1/2}Sc^{1/3}), \quad [7]$$

they expected the enhancement due to convection to be less than 15%.

Although the acoustic streaming in the experiments of Tian and Apfel did not lead to significant enhancement of the evaporative mass transfer, other oscillation methods that cause a higher streaming velocity can greatly increase the mass transfer rate. It is the purpose of this work to examine the enhancement of mass transfer when a charged sphere undergoes periodic oscillation in the surrounding fluid due to an oscillatory electric field. To this end we first examine the governing equations to elucidate the parameters involved and then describe experiments designed to measure evaporative mass transfer from a microdroplet.

A conservative estimate of the enhancement of mass transfer due to particle motion can be obtained by applying quasi-steady-state theory, that is, by assuming that an equation such as Eq. [3] applies at each point in time. The time-average Sherwood number taken over one cycle of oscillation, then, is given by

$$\langle Sh \rangle = \frac{1}{\Delta t} \int_t^{t+\Delta t} [2 + g(t)] dt, \quad [8]$$

in which Δt is the period of one oscillation, and, using Eq. [3] with $n = 3$, the function, $g(t)$, is

$$g(t) = \{ [0.5Pe + 0.3026Pe(t)^2]^{-3} + [1.008Pe(t)^{1/3}]^{-3} \}^{-1/3}, \quad [9]$$

and $Pe(t)$ is based on the time-dependent velocity, $v(t)$. An enhancement factor, E , can be defined by

$$E = \frac{1}{2} \langle Sh \rangle = 1 + \frac{1}{2\Delta t} \int_t^{t+\Delta t} g(t) dt. \quad [10]$$

As shown below, this approach yields enhancement factors much lower than measured. A more rigorous approach for predicting the enhancement and the factors that affect the enhancement is obtained by applying the theory for an oscillating sphere.

THEORY FOR THE OSCILLATING SPHERE

Landau and Lifshitz (13) presented the results for the drag on a sphere that undergoes translatory oscillations in a fluid for creeping flow. If the velocity of the sphere is given by

$$\mathbf{u} = \mathbf{u}_0 e^{-i\omega t}, \quad [11]$$

then the fluid velocity is given by

$$\mathbf{v} = e^{-i\omega t} \nabla \times \nabla \times f(r) \mathbf{u}_0, \quad [12]$$

where $f(r)$ is a function only of radial coordinate r measured from the center of the sphere, and its derivative is given by

$$f' = \frac{df}{dr} = \left[A e^{ikr} \left(r - \frac{1}{ik} \right) + B \right] \frac{1}{r^2}. \quad [13]$$

Here the constants A , B , and k are

$$A = -\frac{3a}{2ik} e^{-ika}, \quad B = -\frac{a^3}{3} \left(1 - \frac{3}{ika} - \frac{3}{k^2 a^2} \right), \quad [14]$$

$$K = \frac{(1+i)}{\sqrt{2\nu/\omega}}.$$

For vertical (z -direction) oscillation with $u_z = u_0 e^{-i\omega t}$ the velocity components of particle motion in spherical coordinates are given by

$$u_r = u_0 e^{-i\omega t} \cos \theta, \quad u_\theta = -u_0 e^{-i\omega t} \sin \theta, \quad u_\phi = 0. \quad [15]$$

Using these velocity components in Eq. [12], the velocity components of the surrounding fluid are

$$v_r = -2u_0 e^{-i\omega t} \frac{f'}{r} \cos \theta, \quad [16]$$

$$v_\theta = u_0 e^{-i\omega t} \left(f'' + \frac{f'}{r} \right) \sin \theta, \quad v_\phi = 0.$$

Introducing f' and f'' based on Eq. [13] in Eq. [16], the fluid velocity components become

$$v_r = -2u_0 e^{-i\omega t} F(r) \cos \theta, \quad v_\theta = u_0 e^{-i\omega t} G(r) \sin \theta, \quad v_\phi = 0, \quad [17]$$

where

$$F(r) = \left[A e^{ikr} \left(r - \frac{1}{ik} \right) + B \right] \frac{1}{r^3}, \quad [18]$$

$$G(r) = \left[A e^{ikr} \left(ikr^2 - r + \frac{1}{ik} \right) - B \right] \frac{1}{r^3}.$$

The convective diffusion equation for the dilute surrounding medium is

$$\frac{\partial c_i}{\partial t} + v_r \frac{\partial c_i}{\partial r} + \frac{v_\theta}{r} \frac{\partial c_i}{\partial \theta}$$

$$= D_{ij} \left[\frac{1}{r^2} \frac{\partial}{\partial r} \left(r^2 \frac{\partial c_i}{\partial r} \right) + \frac{1}{r^2 \sin \theta} \frac{\partial}{\partial \theta} \left(\sin \theta \frac{\partial c_i}{\partial \theta} \right) \right], \quad [19]$$

where c_i is the concentration of the diffusing species in the surrounding fluid. Using Eqs. [17] and [18] and writing $x = \cos \theta$, the convective diffusion becomes

$$\frac{\partial c_i}{\partial t} + u_0 e^{-i\omega t} \left[-2x F(r) \frac{\partial c_i}{\partial r} + (1-x^2) G(r) \frac{\partial c_i}{\partial x} \right]$$

$$= \frac{D_{ij}}{r^2} \left[\frac{\partial}{\partial r} \left(r^2 \frac{\partial c_i}{\partial r} \right) + \frac{\partial}{\partial x} \left((1-x^2) \frac{\partial c_i}{\partial x} \right) \right]. \quad [20]$$

It is convenient to write this governing equation in nondimensional form by introducing the dimensionless quantities

$$\tau = \frac{D_{ij} t}{a^2}, \quad \xi = \frac{r}{a}, \quad \Phi = \frac{c_i}{c_{i,a}}, \quad \text{Pe}_0 = \frac{2au_0}{D_{ij}}, \quad [21]$$

where $c_{i,a}$ is the interfacial concentration of the diffusing species. Using these variables, Eq. [20] transforms to

$$\frac{\partial \Phi}{\partial \tau} + \frac{\text{Pe}_0}{2} e^{-i\omega a^2 \tau / D_{ij}} \left[-2x F(\xi) \frac{\partial \Phi}{\partial \xi} + (1-x^2) G(\xi) \frac{\partial \Phi}{\partial x} \right]$$

$$= \frac{1}{\xi^2} \left\{ \frac{\partial}{\partial \xi} \left(\xi^2 \frac{\partial \Phi}{\partial \xi} \right) + \frac{\partial}{\partial x} \left[(1-x^2) \frac{\partial \Phi}{\partial x} \right] \right\}, \quad [22]$$

where

$$F(\xi) = \left[\frac{3}{2} e^{ika(1-\xi)} \left(\frac{1}{k^2 a^2} - \frac{\xi}{ika} \right) - \frac{1}{3} + \frac{1}{ika} + \frac{1}{k^2 a^2} \right] \frac{1}{\xi^3}, \quad [23]$$

and

$$G(\xi) = \frac{3}{2} e^{-ika(1-\xi)} \left(\frac{1}{k^2 a^2} + \frac{\xi}{ika} - \xi^2 \right) \frac{1}{\xi^3}. \quad [24]$$

This result shows that the concentration in the surrounding fluid depends on three dimensionless parameters (i) ka , (ii) the maximum Peclet number, Pe_0 , and (iii) an oscillation parameter, $\omega a^2 / D_{ij}$, that represents the ratio of the diffusion time scale to

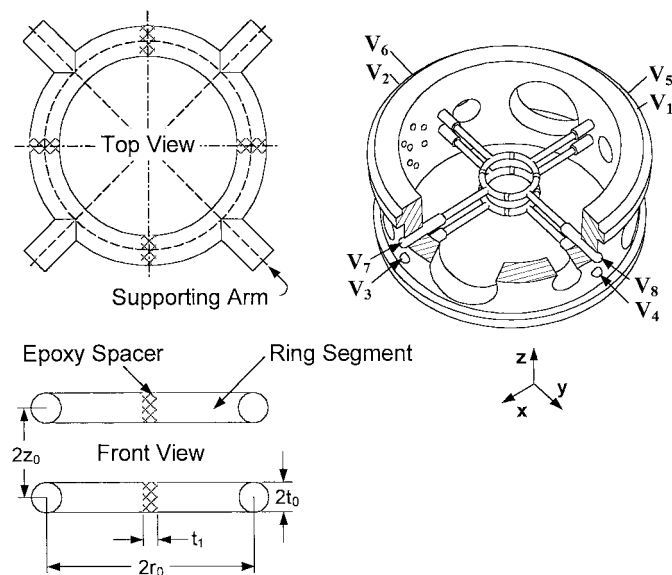


FIG. 2. The octopole EDB electrode configuration. Each ring is composed of four segments providing X and Y dc control as well as vertical dc control (ring half-spacing $z_0 = 1.98$ mm, ring radius $r_0 = 5.56$ mm, ring half-thickness $t_0 = 0.794$ mm, epoxy spacer thickness $t_1 = 0.794$ mm).

the oscillation time scale. These parameters govern the mass transfer characteristics of the oscillating microspheres.

If the diffusion time scale, a^2/D_{ij} , is small compared with oscillation time scale, ω^{-1} , vapor will diffuse at a greater rate from the neighborhood of the oscillating particle during one cycle than it would for a stagnant system. An increased mass

transfer rate can also be expected as the Peclet number increases due to convective diffusion. The parameter ka relates to the viscous damping of the particle motion.

EXPERIMENTS

Experiments were performed using an octopole double ring electrodynamic balance (EDB) described by Zheng *et al.* (14). The electrode configuration is shown in Fig. 2. This design permits three-dimensional control of the particle position by adjusting the dc potential on each of the ring sections.

The electrodes were mounted in a stainless-steel chamber that had several optical ports for mounting the peripheral equipment shown in an overhead view in Fig. 3. By superposition of ac and dc potentials applied to the two electrodes, a droplet can be levitated at rest or can be oscillated in either of two modes. If the ac potential is below a certain critical potential, stable harmonic oscillation at the frequency of the ac field can be achieved by increasing or decreasing the dc potential from the value required to balance the gravitational force. The amplitude of the oscillation is proportional to this dc "offset voltage."

As shown in the analysis of the equation of motion of a levitated particle in an EDB by Frickel *et al.* (15), the frequency of the oscillation is either that of the ac drive or one-half that frequency, depending on the ac field strength and the fluid mechanical drag on the particle. If the ac potential is above the so-called springpoint potential, large-amplitude oscillation occurs at half the frequency of the ac drive frequency. The dynamics of a charged particle in an EDB were analyzed by a number of investigators (15–19). These analyses show that, in the absence

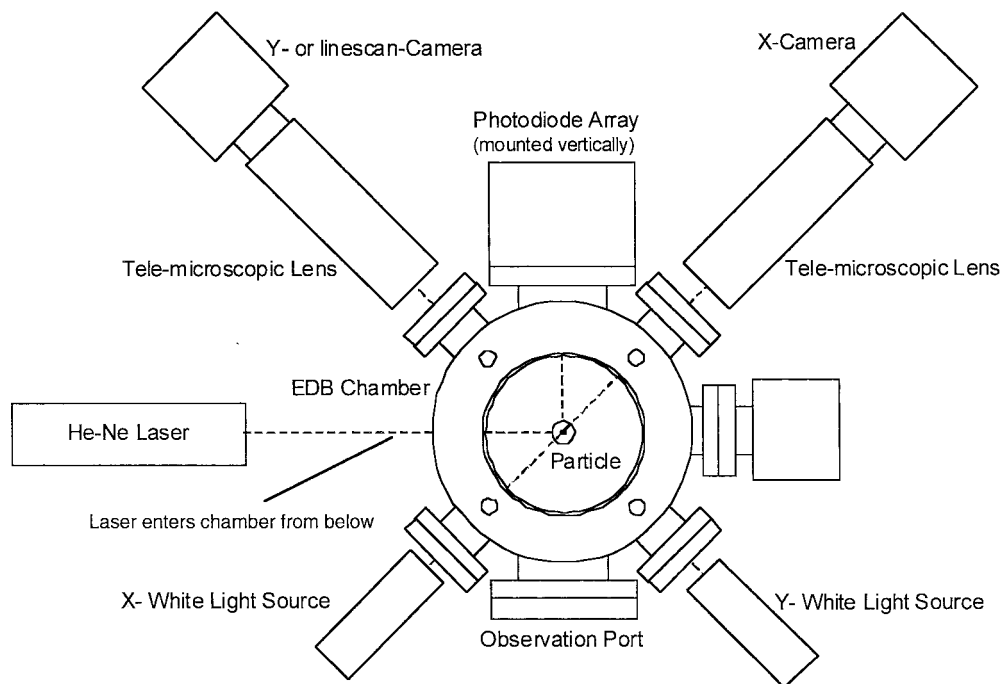


FIG. 3. Overview of the EDB system looking from the top of the experimental setup.

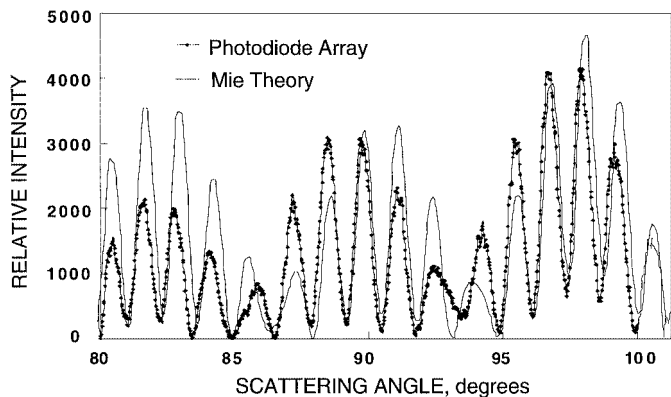


FIG. 4. Angular scattering data for a 30.4- μm -diameter dodecanol droplet compared with Mie theory.

of a dc bias in the vertical direction, three dimensionless parameters govern the stability characteristics. These are the drag parameter, δ , ac field strength parameter, β , and the dc imbalance parameter, σ , defined by

$$\delta = \frac{12\pi\mu R}{m\omega}, \quad \beta = \frac{2g}{\omega^2 b} \left(\frac{V_{ac}}{V_{dc,0}} \right), \quad \sigma = \frac{4g}{\omega^2 b} \left(\frac{V_{dc} - V_{dc,0}}{V_{dc,0}} \right), \quad [25]$$

in which m is the particle mass, V_{dc} is the dc potential, $V_{dc,0}$ is the dc potential necessary to balance the particle weight, V_{ac} is the ac potential, μ is the gas viscosity, and g is the gravitational acceleration constant. The balance “length,” b , is defined by $b = z_0 C_0 / C_1$, in which z_0 is the half the separation between rings, and C_0, C_1 are other experimentally determined constants for the EDB. It is assumed that particle motion is in the Stokes flow regime.

The lowest marginal stability envelope (springpoint) is given by Müller’s approximation (19) for the critical value of β ; that is,

$$\beta_{crit} = \frac{1}{2}(99 + 12\delta^2) - \sqrt{\frac{1}{4}(99 + 12\delta^2)^2 - (1 + 4\delta^2)(81 + 36\delta^2)}. \quad [26]$$

For $\beta > \beta_{crit}$ the particle undergoes a large-amplitude oscillation at one-half the frequency of the ac drive. If β is too large, the particle can be lost, so the ac potential and the drive frequency must be selected to avoid particle loss.

As depicted in Fig. 3 the trapped particle was illuminated either by a He-Ne laser or by a white light source. The He-Ne laser entered the EDB chamber from an optical port at the bottom. To size the microsphere, the angular (Mie) scattering was recorded with a photodiode array (PDA) mounted vertically on one of the chamber ports at 90° to the scattering plane. The particle size was determined by comparing the PDA data (angles from 78 to 102°) with Mie theory calculations over the same angle range. An example of the fit for a 30.4- μm -diameter dodecanol droplet is shown in Fig. 4; the measured scattered intensity profile is seen to be in agreement with Mie theory with respect to the angular positions of peaks and troughs. The peak amplitudes vary

somewhat from Mie theory computations. Since the array was not cooled, the disagreement is due partly to noise and partly to the fact that the pixels were not calibrated to take into account variations in the optical efficiency of the detector elements.

Two CCD video cameras with 9.45x telemicroscopic lenses were mounted on ports directly opposite white light sources to obtain shadow images of the particle in two dimensions. Figure 5a is an image of a stationary 42- μm -diameter dodecanol

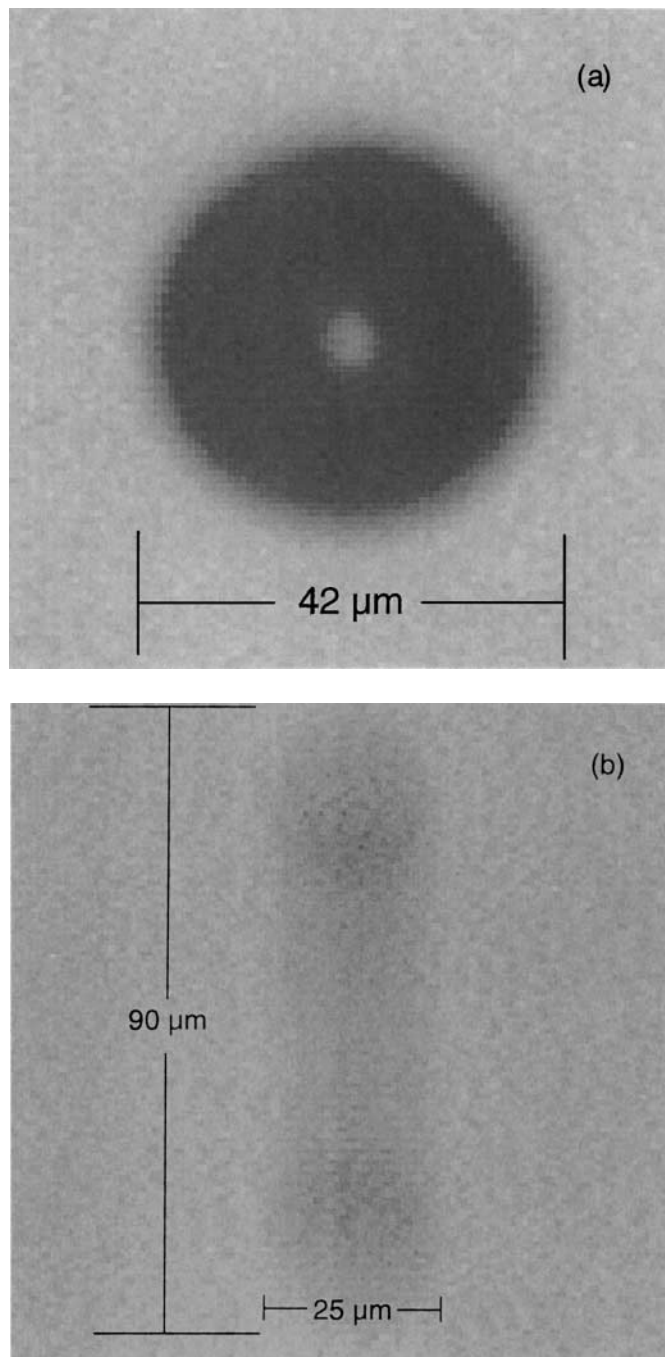


FIG. 5. (a) Video image of a stationary dodecanol microdroplet with a diameter of 42 μm , and (b) a video image of a microparticle oscillating stably at small amplitude.

particle just after it was trapped in the EDB. The video images recorded during oscillation showed that no distortion of the droplet from spherical occurred.

The trajectory of the oscillating particle was recorded with a CCD linescan camera (Reticon) mounted in place of the X-camera (using the same telemicroscopic lens). The camera had a single line of 256 pixels aligned in the vertical direction. The He-Ne laser beam cast a shadow of the trapped particle on the camera and as the particle oscillated, its magnified shadow covered different groups of pixels at different times. The resulting pixel gray-scale profile was, therefore, time-dependent and was used to determine the particle position as a function of time. Figure 5b is a video (shadow) image of a microparticle oscillating with a stable small amplitude.

Representative particle trajectories of large amplitude springpoint oscillation and small amplitude stable oscillation are shown in Fig. 6. When the particle goes from a condition of stable oscillation to oscillation above the springpoint, the frequency changes from the drive frequency to one-half the drive frequency. Furthermore, the large-amplitude oscillation is not sinusoidal because the vertical electric field driving the particle motion is nonuniform, but the small-amplitude oscillation around the midplane is nearly sinusoidal because the electric field is almost uniform near the midplane. The particle trajectory during the large-amplitude oscillation is approximately a "saw tooth."

Particle velocities corresponding to the trajectories shown in Fig. 6 are presented in Fig. 7. The velocities associated with large-amplitude oscillations are significantly distorted from simple harmonic motion compared with those for small-amplitude oscillations. The largest velocity encountered was 0.343 m s^{-1} for a $40.3\text{-}\mu\text{m}$ -diameter droplet. This corresponds to a maximum Reynolds number of about 0.91, and a mean Reynolds number for one cycle of 0.45. The mean Reynolds numbers ($\langle \text{Re} \rangle = 2a\langle |u| \rangle / \nu$ based on the mean speed, $\langle |u| \rangle$, for one cycle) varied from 0.083 to 0.45 for the data presented below, and the maximum Peclet numbers ($\text{Pe}_0 = 2au_0/D_{ij}$) varied from 0.369

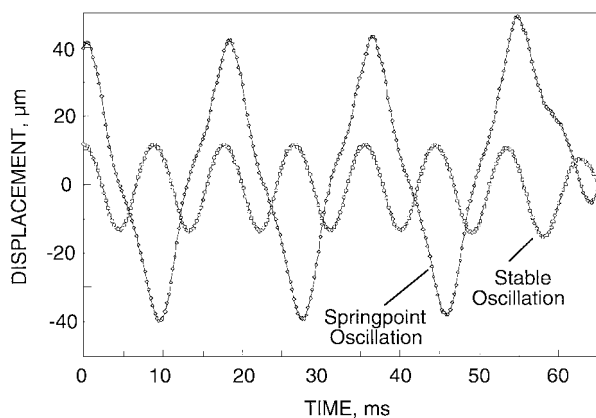


FIG. 6. Oscillation trajectories of dodecanol droplets. For stable oscillation $f = 111.0 \text{ Hz}$, and for springpoint oscillation $f = 110.6 \text{ Hz}$.

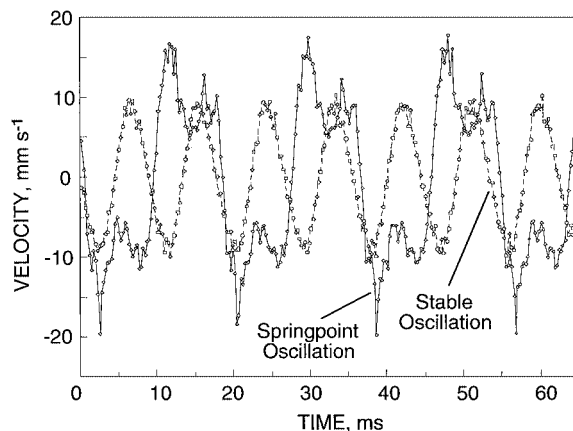


FIG. 7. Particle velocities corresponding to the trajectories of Fig. 6.

to 2.60. The largest Reynolds numbers encountered here are somewhat beyond the range where creeping flow is rigorously applicable, but for oscillations in the stable region of the stability map creeping flow is a reasonable approximation. For stable oscillation the largest mean Reynolds number was 0.323. For colloidal particles involving very low Reynolds numbers ($\text{Re} \ll 1$), the general result that the mass transfer is characterized by ka , a Peclet number and $\omega a^2/D_{ij}$ should certainly apply.

MASS TRANSFER RESULTS

Dodecanol has a low vapor pressure, and simultaneous application of Eqs. [3] and [5] indicates that evaporation is very close to isothermal, that is, $T_a \sim T_\infty$. In our experiments nitrogen was passed through the EDB chamber to remove vapor and maintain $p_\infty \sim 0$. In this case Eq. [5] reduces to

$$a^2 = a_0^2 - \frac{2D_{ij}M_i p_i^0(T_\infty)}{\rho RT_\infty}(t - t_0). \quad [27]$$

This result corresponds to an interfacial mass flux, j_a , given by

$$j_a = \frac{D_{ij}}{a} \frac{M_i p_i^0(T_\infty)}{RT_\infty}. \quad [28]$$

When there is gas phase convection the interfacial mass flux may be written as

$$j_a = K_G \frac{M_i p_i^0(T_\infty)}{RT_\infty}, \quad [29]$$

and Eq. [27] becomes

$$a^2 = a_0^2 - \frac{2K_G a M_i p_i^0(T_\infty)}{\rho RT_\infty}(t - t_0). \quad [30]$$

Based on Eq. [27], a graph of a^2 versus time should yield a straight line with slope, $S_0 = -2D_{ij}M_i p_i^0(T_\infty)/\rho RT_\infty$ provided

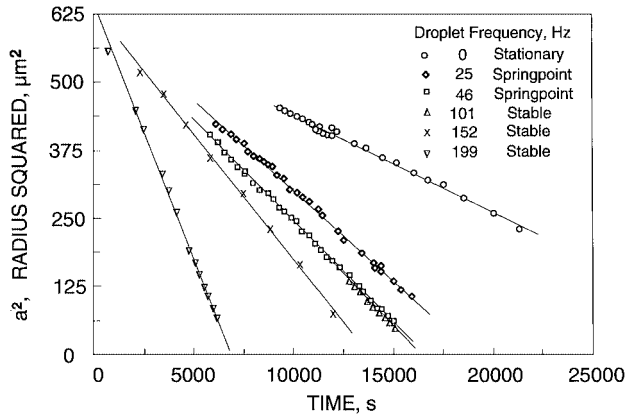


FIG. 8. Evaporation data for dodecanol droplets for various oscillation frequencies.

that the process proceeds isothermally. The ratio of the slope of the equation with gas convection (Eq. [30]) to the slope of the equation for mass transfer to a stagnant medium (Eq. [27]) defines the mass transfer enhancement factor and is given by

$$E = S/S_0 = K_G a / D_{ij}. \quad [31]$$

Figure 8 presents the results for several experiments at 295 K for dodecanol droplet evaporation plotted as a^2 versus time. A least-squares fit to the data gives a slope of $-0.0180 \mu\text{m}^2 \text{s}^{-1}$ for a stationary particle, and for various conditions of oscillation the absolute values of the slopes are greater than this limiting case. This slope is in good agreement with results reported by Taflin *et al.* (20) for dodecanol evaporation in N_2 at 295 K, which is $S_0 = -0.0190 \mu\text{m}^2 \text{s}^{-1}$. The largest slope ($-0.0938 \mu\text{m}^2 \text{s}^{-1}$) was measured for a stably oscillating particle at the largest frequency ($f = 199 \text{ Hz}$). As would be expected, the particles oscillating at lower frequencies had lower mass transfer rates. The other stably oscillating particles at frequencies of 150 and 100 Hz had slopes of -0.0463 and $-0.0382 \mu\text{m}^2 \text{s}^{-1}$, respectively. The particles oscillating at the springpoint had lower slopes, -0.0372 and $-0.0332 \mu\text{m}^2 \text{s}^{-1}$, for 46 and 25 Hz, respectively.

The slopes of the data obtained with and without oscillation are essentially linear. Consequently, $K_G a$ is constant for each

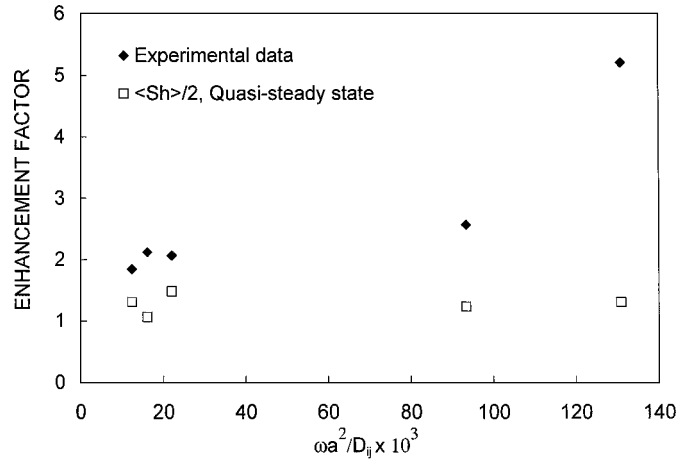


FIG. 9. The mass transfer enhancement factor as a function of dimensionless parameter $\omega a^2 / D_{ij}$.

run, and the enhancement factor is a constant for each experiment over the range of sizes studied. The largest enhancement factor ($E = 5.20$) corresponds to the small-amplitude experiment with the highest frequency ($f = 199 \text{ Hz}$) and an initial radius $a_0 = 23.6 \mu\text{m}$. This also corresponds to the lowest Reynolds number encountered, the mean value being $\langle \text{Re} \rangle = 0.083$.

Figure 9 is a plot of the enhancement factors versus $\omega a^2 / D_{ij}$ for the experiments. The large amplitude oscillations, which were also at the lowest frequency, have smaller enhancement factors than the high frequency small amplitude oscillations. Although the theory outlined above indicates that the governing parameters are $\omega a^2 / D_{ij}$, ka , and Pe_0 , the most significant parameter here is $\omega a^2 / D_{ij}$, which varied from 12.4 to 131. The variations in ka and Pe_0 were smaller [$0.0466 \leq ka / (1 + i) \leq 0.151$ and $0.369 \leq \text{Pe}_0 \leq 2.60$].

In Fig. 9 calculated values for $\langle \text{Sh} \rangle / 2$, based on quasi-steady motion using the integral in Eq. [10], are plotted for each value of $\omega a^2 / D_{ij}$. To calculate the Peclet number for each frequency, the measured velocities and the average radius of the droplet during the experiment were used. As can be seen, the enhancement factors based on quasi-steady motion are substantially lower than the measured values.

TABLE 1
Experimental Conditions and Measured Enhancement Factors

| Initial diameter (μm) | Motion type | Max speed (m s^{-1}) | Frequency (Hz) | Measured enhancement $E = S/S_0$ | Calculated enhancement, $E = \langle \text{Sh} \rangle / 2$ | | $\omega a^2 / D_{ij}$ ($\times 10^2$) |
|---------------------------------------|--------------------|------------------------------------|-------------------|--|--|---------|--|
| | | | | | Minimum | Maximum | |
| 42.1 | Stationary | 0 | 0 | 1 | 1.0 | 1.0 | 0 |
| 40.9 | Springpoint | 0.187 | 25.0 | 1.84 | 1.15 | 1.31 | 12.4 |
| 40.3 | Springpoint | 0.343 | 45.9 | 2.07 | 1.22 | 1.48 | 22.0 |
| 23.3 | Stable oscillation | 0.084 | 101.0 | 2.12 | 1.04 | 1.07 | 16.2 |
| 45.5 | Stable oscillation | 0.127 | 152.2 | 2.57 | 1.07 | 1.23 | 93.4 |
| 47.2 | Stable oscillation | 0.163 | 198.7 | 5.2 | 1.01 | 1.31 | 131 |

The diffusion coefficient used to calculate the Sherwood number was estimated from the semitheoretical equation of Fuller *et al.* (21), which is based on Chapman-Enskog theory for low density gases. The estimated diffusivity at 295 K and atmospheric pressure is $D_{ij} = 5.31 \times 10^{-6} \text{ m}^2 \text{ s}^{-1}$.

Table I summarizes the experimental conditions and enhancement factors. The frequencies reported are the particle oscillation frequencies. For large-amplitude oscillations above the springpoint the particle frequencies are one-half the ac drive frequency. Since the droplet radius changed during an experiment, the Sherwood number based on the size during one cycle near the beginning of a run differed from that at the end of a run. Consequently, maximum and minimum enhancement factors ($(Sh)/2$) calculated using Eq. [10] and the quasi-steady-flow assumption were computed for conditions near the beginning and near the end of each experimental run.

COMMENTS

We have demonstrated that particle oscillation can substantially increase mass transfer rates between a small sphere and the surrounding fluid. Although this was demonstrated for the evaporation of single dodecanol droplets in nitrogen, the results should be applicable to mass transfer in colloidal systems as well as aerocolloidal systems. Based on these observations one can expect that the rates of processes involving mass transfer between a colloidal particle and a surrounding fluid can be substantially increased by oscillating the particles.

Although, for the limited range of frequencies used here, no maximum in the enhancement factor was reached as the frequency increased, one can expect a maximum to occur when the time scale for diffusion is of the order of the time scale of the oscillation. For a 40- μm -diameter droplet the time scale for diffusion is $a^2/D_{ij} = 0.0753 \text{ ms}$. For the highest frequency, $f \approx 200 \text{ Hz}$, the time scale of the oscillation is $\omega^{-1} = (2\pi f)^{-1} = 0.8 \text{ ms}$. Thus, one can expect the enhancement factor to decrease when $a^2/D_{ij} > \omega^{-1}$. In this case there is insufficient time for diffusion to occur during one cycle of oscillation.

The relatively low mass transfer enhancements reported by Tian and Apfel using acoustic oscillation appear to be due to much lower streaming velocities than encountered here.

ACKNOWLEDGMENTS

The authors are grateful to NSF for Grant CTS-9982413 and to the National Natural Science Foundation of China for Grants 29876022 and 29976026 that supported this research.

REFERENCES

1. Maxwell, J. C., in "Encyclopaedia Britannica," 9th ed., Vol. 7, p. 214, 1878.
2. Wagner, P. E., in "Aerosol Microphysics II. Chemical Physics of Microparticles" (W. H. Marlow, Ed.), Vol. 29, p. 129. Springer-Verlag, Berlin, 1982.
3. Kulmala, M., and Vesala, T., *J. Aerosol Sci.* **22**, 337 (1991).
4. Kronig, R., and Bruijsten, J., *Appl. Sci. Res.* **A2**, 439 (1951).
5. Acrivos, A., and Taylor, T. D., *Phys. Fluids* **5**, 387 (1962).
6. Rimmer, P. L., *J. Fluid Mech.* **32**, 1 (1968).
7. Rimmer, P. L., *J. Fluid Mech.* **35**, 827 (1969).
8. Tafin, D. C., and Davis, E. J., *Chem. Eng. Commun.* **55**, 199 (1987).
9. Zhang, S. H., and Davis, E. J., *Chem. Eng. Commun.* **50**, 51 (1987).
10. Levich, V. G., "Physicochemical Hydrodynamics." Prentice-Hall, New York, 1962.
11. Tian, Y., and Apfel, R. E., *J. Aerosol Sci.* **27**, 721 (1996).
12. Rosner, D. E., "Transport Processes in Chemically Reacting Flow Systems." Butterworths, Boston, 1986.
13. Landau, L. D., and Lifshitz, E. M., "Fluid Mechanics." Pergamon, Oxford, 1959.
14. Zheng, F., Qu, X., and Davis, E. J., *Rev. Sci. Instrum.* **72**, 3380 (2001).
15. Frickel, R. H., Shaffer, R. E., and Stamatoff, J. B., Report No. ARCSL-TR-77041, Chemical Systems Laboratory, Aberdeen Proving Ground, MD, 1978.
16. Davis, E. J., *Langmuir* **1**, 379 (1985).
17. Iwamoto, T., Itoh, M., and Takahashi, K., *Aerosol Sci. Technol.* **15**, 127 (1991).
18. Hartung, W. H., and Avedisian, C. T., *Proc. Roy. Soc.* **437**, 237 (1992).
19. Müller, A., *Ann. Phys.* **6**, 206 (1960).
20. Tafin, D. C., Zhang, S. H., Allen, T., and Davis, E. J., *AIChE J.* **34**, 1310 (1988).
21. Fuller, E. N., Schettler, P. D., and Giddings, J. C., *Ind. Eng. Chem.* **58**, 19 (1966).